Proceedings of ICAPP '12
Chicago, USA, June 24-28, 2012
Paper 12049

Experimental Results of the QUENCH-16 Bundle Test on Air Ingress

J. Stuckert, M. Steinbrück
Karlsruhe Institute of Technology (KIT)
Hermann-von-Helmholtz-Platz 1, 76344 Eggenstein-Leopoldshafen
Tel: +49 721 608 22558 , Fax: +49 721 608 23956 , Email: juri.stuckert@kit.edu

Abstract – *The out-of-pile bundle experiment QUENCH-16 on air ingress was conducted in the electrically heated 21-rod QUENCH facility at KIT in July 2011. It was performed in the frame of the EC supported LACOMECO program. The test scenario included the oxidation of the Zircaloy-4 claddings in air following a limited pre-oxidation in steam, and involved a long period of oxygen starvation to promote interaction with the nitrogen. The primary aim was to examine the influence of the formed oxide layer structure on bundle coolability and hydrogen release during the terminal flooding phase. QUENCH-16 was thus a companion test to the earlier air ingress experiment, QUENCH-10, which was performed with strongly pre-oxidized bundle. Unlike QUENCH-10, significant temperature escalation and intensive hydrogen release were observed during the reflood phase. Post-test investigations of bundle cross sections reveal residual nitride traces at various elevations. The external part of the oxide scale is of porous structure due to re-oxidation of nitrides during reflood. Relative thick internal oxide scales underneath this porous layer and residual nitrides were formed during reflood. At lower bundle elevations frozen partially oxidized melt was detected, relocated from upper elevations.*

I. INTRODUCTION

Air ingress issues have received considerable attention in recent years in view of the likely acceleration in cladding oxidation, fuel rod degradation, and the release of some fission products, most notable ruthenium. The Paks NPP cleaning tank incident and the accidents at Fukushima Daiichi drew attention to the possibility of overheated fuel assemblies becoming exposed to air outside of the reactor.

Experimental and analytical works on air ingress were performed within the EC 4th and 6th Framework Programs[1, 2]. Numerous single effect tests on cladding oxidation in air were performed at ANL[3] (temperatures 573–1173 K), AEKI[4] (temperatures 873–1773 K), and KIT[5, 6] (temperatures 873–1873 K). The current OECD/NEA project SFP investigates the performance of full-scale 17x17 PWR assemblies in air with regard to thermal-hydraulic and ignition phenomena[7]. A number of previous bundle air ingress tests have been performed under a range of configurations and oxidizing conditions, namely CODEX AIT-1, AIT-2[8], QUENCH-10[9, 10] and PARAMETER[11]-SF4[12]. The accumulated data have demonstrated that air oxidation of cladding is a quite complex phenomenon governed by numerous processes depending on the oxidizing conditions, the oxidation history and the details of the cladding material specification. The models for air oxidation do not yet cover the whole range of representative conditions. The main aims of new bundle tests should be the investigation of areas where data were mostly missing.

The QUENCH-16 bundle test was proposed by AEKI in the frame of the EC-sponsored LACOMECO program[13] as part of the collective investigation of air ingress into overheated nuclear fuel assemblies. The experiment focused specifically on the following phenomena:

- air oxidation after rather moderate pre-oxidation in steam;
- slow oxidation and nitriding of cladding in high temperature air and transition to rapid oxidation and temperature excursion;
- role of nitrogen under oxygen-starved conditions;
- formation of oxide and nitride layers on the surface of cladding;
- reflooding of the oxidized and nitrided bundle by water, release of hydrogen and nitrogen.

The proposal included a target scenario characterized by:

- a long period of oxygen starvation to promote the appearance of the above mentioned phenomena;
- reflood quench initiated at temperatures well below the melting point of the cladding to provide the opportunity of avoiding a major oxidation, to facilitate post-test inspection of the bundle.

Concerning the second objective, it was realized that avoiding such an excursion could not be guaranteed, especially in the light of previous experiments such as PARAMETER-SF4 which showed clearly how a starvation

period can promote an excursion. The outcome would in any case yield valuable data on this phenomenon.

QUENCH-16 was successfully performed on 27 July 2011, according to a test protocol agreed following discussions among the participants and based on coordinated planning analyses by GRS, EDF and PSI using independent simulation tools.

II. TEST FACILITY AND INSTRUMENTATION

The main component of the QUENCH test facility is the test section with the test bundle (Fig. 1).

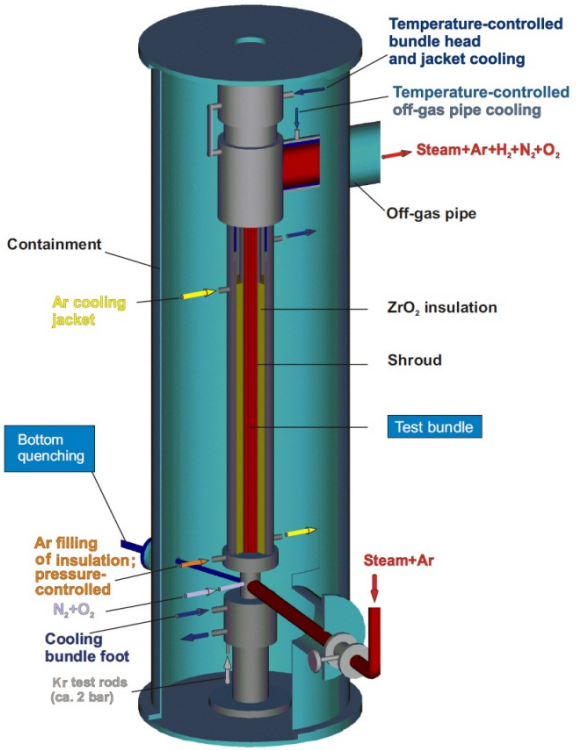

Fig. 1. QUENCH Facility: Containment and test section.

The facility can be operated in two modes: a forced-convection mode (typical for most QUENCH experiments) and a boil-off mode. QUENCH-16 was conducted in forced-convection mode, in which superheated steam from the steam generator and superheater together with argon as a carrier gas for off-gas measurements enter the test bundle at the bottom. The system pressure in the test section is around 0.2 MPa absolute. The test section has separate inlets at the bottom to inject water for reflood (bottom quenching) and synthetic air (80% N_2 + 20% O_2) during the air ingress phase. The argon, the steam and gases not consumed, and the hydrogen produced in the zirconium-steam reaction flow from the bundle outlet at the top through a water-cooled off-gas pipe to the condenser where the steam is separated from the non-condensable gases. The water cooling circuits for bundle head and off-gas pipe are temperature-controlled to guarantee that the steam/gas temperature is high enough so that condensation at the test section outlet and inside the off-gas pipe is avoided.

The test bundle is approximately 2.5 m long and is made up of 21 fuel rod simulators (Fig. 2). The fuel rod simulators with the Zircaloy-4 (Zry-4) claddings are held in position by five grid spacers, four are made of Zry-4 and the one at the bottom of Inconel 718. Except the central one all rods are heated. Heating is electric by 6 mm diameter tungsten heaters of length 1024 mm installed in the rod centre (lower edge of heaters corresponds to bundle elevation 0 mm). Electrodes of molybdenum (length 300 + 576 mm; Ø 8.6 mm) and copper (length 390 + 190 mm; Ø 8.6 mm) are connected to the tungsten heaters at one end and to the cables leading to the DC electrical power supply at the other end. The heating power is distributed between two groups of heated rods. The distribution of the electric power within the two groups is as follows: about 40% of the power is released into the inner rod circuit consisting of eight fuel rod simulators (in parallel connection) and 60% in the outer rod circuit (12 fuel rod simulators in parallel connection).

The tungsten heaters are surrounded by annular ZrO_2-TZP pellets. The rod cladding of the heated and unheated fuel rod simulators is Zry-4 with 10.75 mm outside diameter and 0.725 mm wall thickness. All test rods are filled with Kr at a pressure of approx. 0.22 MPa absolute. The rods were connected to a controlled feeding system that compensated minor gas losses and allowed observation of the first cladding failure as well as a failure progression.

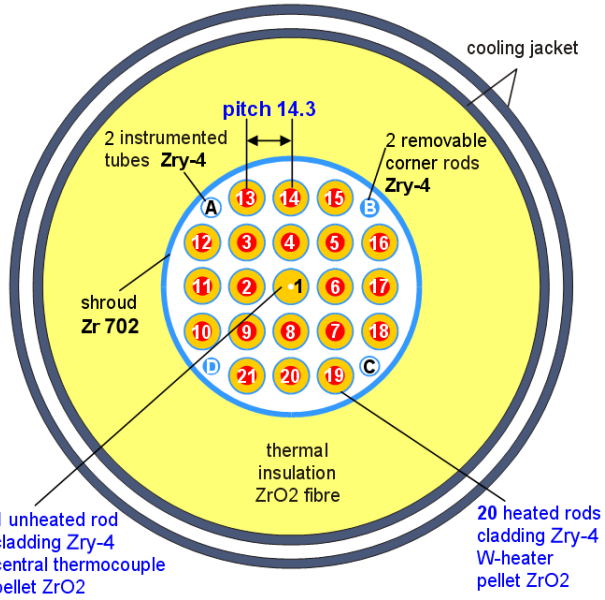

Fig. 2. Bundle cross-section with marked rods.

There are four corner rods installed in the bundle. Two of them, i.e. rods "A" and "C", are made of a Zircaloy-4 solid rod at the top and a Zircaloy-4 tube at the bottom and are used for thermocouple instrumentation. The other two rods, i.e. rods "B" and "D" (solid Zircaloy-4 rods of 6 mm diameter) are particularly designed to be withdrawn from the bundle to check the amount of oxidation and hydrogen uptake at specific times. Rod B was pulled out of the bundle before the air ingress phase of the experiment and rod D was pulled before quenching; low part of rod A was removed after test termination.

The test bundle is surrounded by a 3.05 mm shroud of Zirconium-702 (inner diameter 82.8 mm) with a 34 mm thick ZrO_2 fiber insulation extending from the bottom to the upper end of the heated zone and a double-walled cooling jacket of Inconel (inner tube) and stainless steel (outer tube) over the entire length. The annulus between shroud and cooling jacket is purged (after several cycles of evacuation) and then filled with stagnant argon at 0.22 MPa absolute. The annulus is connected to a flow- and pressure-controlled argon feeding system in order to keep the pressure constant at the target of 0.22 MPa and to prevent an access of steam to the annulus after shroud failure. The 6.7-mm annulus of the cooling jacket is cooled by argon flow from the upper end of the heated zone to the bottom of the bundle and by water in the upper electrode zone. Both the absence of ZrO_2 insulation above the heated region and the water cooling are to avoid too high temperatures of the bundle in that region.

The test bundle, shroud, and cooling jacket are extensively equipped with sheathed thermocouples at different elevations with an axial step width of 100 mm. The thermocouples in the hot zone and above are high-temperature thermocouples with W5Re/W26Re wires, HfO_2 insulation, and a duplex sheath of tantalum (inside) and Zircaloy (outside) with an outside diameter of about 2.2-2.3 mm. The thermocouples in the lower bundle region, i.e. up to 550 mm elevation, are NiCr/Ni thermocouples with stainless steel sheath/MgO insulation and an outside diameter of 1.0 mm used for measurements of the rod cladding and shroud temperatures.

There are 40 high-temperature (W/Re) thermocouples in the upper hot bundle region (bundle and shroud thermocouples between elevations 650 and 1350 mm) and 32 low-temperature (NiCr/Ni) thermocouples in the lower "cold" bundle region (bundle and shroud thermocouples between -250 and 550 mm). The thermocouples attached to the outer surface of the rod cladding at elevations between -250 and 1350 mm are designated "TFS" for all heated rods and "TCR" for the centre unheated rod. At elevations 950 and 650 mm there are two centerline high-temperature thermocouples in the central rod (designation "TCRC"), which are protected from oxidizing influence of steam and air. Two other protected high temperature thermocouples are installed at elevations 950 and 850 mm inside the corner rods A and C and designated "TIT". The shroud thermocouples (designation "TSH") are mounted at the outer surface between 250 and 1250 mm. Additionally, the test section incorporates pressure gauges, flow meters, and a water level detector.

The off-gas including Ar, H_2, O_2, N_2 and steam is analyzed by a state-of-the-art mass spectrometer Balzers "GAM300" whose sampling position is located at the off-gas pipe ≈2.66 m downstream the test section. The mass spectrometer allows also indicating the failure of rod simulators by detection of Kr release.

III. TEST CONDUCT AND PERTINENT RESULTS

The test was performed with a bundle similar to that used in the QUENCH-10. The experience of the QUENCH-10 test provided very valuable information for test preparation and for this reason the QUENCH-16 scenario was specified with the modification of QUENCH-10 scenario. Two important changes were considered in the QUENCH-16 scenario:

- The pre-oxidation period was shortened compared to QUENCH-10 to produce thinner (100-200 µm instead of 500 µm) oxide scale on the cladding. The oxidation temperature and power were kept similar to QUENCH-10.
- The air ingress phase lasted longer and the maximum temperature was lower than in QUENCH-10. During the specification of the test conditions it was emphasized that oxygen starvation should be established in the upper part of the bundle. To reach such conditions the power and the air flow rate were reduced and the argon flow rate was increased. It was proposed to have an average heat-up rate in this phase between 0.1-0.2 K/s.

In summary the QUENCH-16 test was conducted with the following tests phases:

Prepara-tion	Heat-up to peak cladding temperature T_{pct} = 873 K
Phase I	Stabilization at 873 K; facility checks
Phase II	Heat-up with 0.1-0.4 K/s to 1300 K during 2300 s
Phase III	Pre-oxidation of the test bundle in a flow of 3.3 g/s superheated steam and 3 g/s argon during 4000 s at temperatures increasing from 1300 K to 1430 K
Phase IV	Intermediate cooling from 1430 K to 1000 K during 1000 s in the same flow of steam and argon to achieve an adequate duration of the subsequent air ingress phase.
Phase V	Air ingress and transient heat-up from 1000 K to 1873 K with slow heating rate of 0.2 K/s in a flow of 0.2 g/s of air for 4040 s. Total oxygen consumption during 835 s before end of this phase.
Phase VI	Quenching of the bundle by a flow of 50 g/s of water. Temperature escalation to 2420 K with intensive hydrogen release.

Fig. 3 illustrates the phases of the QUENCH-16 test performance. In the pre-oxidation phase and following slow cooling phase the claddings were oxidized in superheated steam (3.3 g/s). 14.3 g hydrogen were released during these two test phases. The maximal thickness of the ZrO_2 layer for withdrawn rod B was 135 µm.

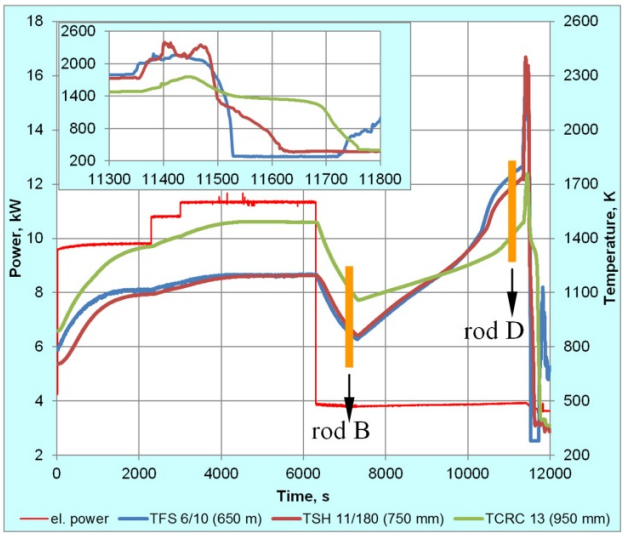

Fig. 3. Test conduct: power input and selected temperatures.

In the subsequent air ingress phase, which lasted 4035 s, the steam flow was replaced by 0.2 g/s of air. The residual steam was exhausted during about 1000 s and caused release of 1.3 g hydrogen. The change in flow conditions had the immediate effect of reducing the heat transfer so that the temperatures began to rise again. After some time measurements demonstrated gradually an increasing consumption of oxygen, accompanied by acceleration of the temperature increase at certain locations. The faster increase was most marked at the mid elevations of the bundle (Fig. 4).

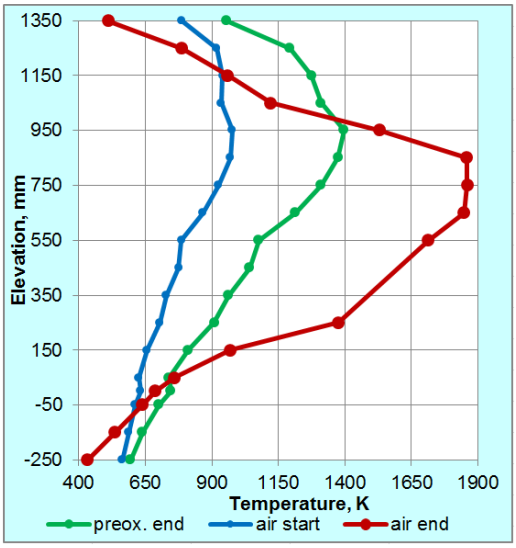

Fig. 4. Change of axial temperature profile during test.

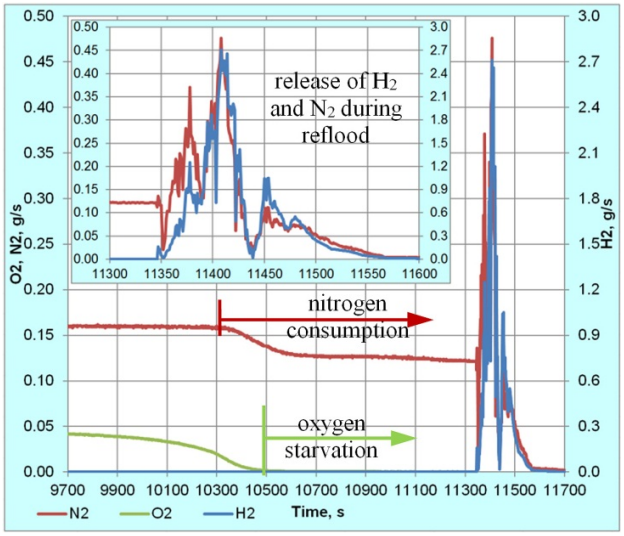

Fig. 5. QUENCH-16 mass spectrometer analysis of off-gas.

Oxygen was completely consumed at about 3200 s after beginning of air ingress (Fig. 5). Shortly before that time, partial consumption of the nitrogen was first observed, indicating local oxygen starvation which promoted the onset of nitriding. Following this, the temperature continued to increase until water injection was initiated when the maximum observed temperature was ca. 1873 K. Thus there was a period of about 835 s complete oxygen consumption and hence starvation in at least part of the bundle. The total uptakes of oxygen and nitrogen were about 58 and 29 g, respectively. The generally limited rate of temperature increase was the result of a rather low air flow rate, probably not untypical of reactor or spent fuel pool conditions.

Metallographic investigations of corner rod D, withdrawn before reflood initiation, showed formation of porous nitrides inside the oxide layer (Fig. 6).

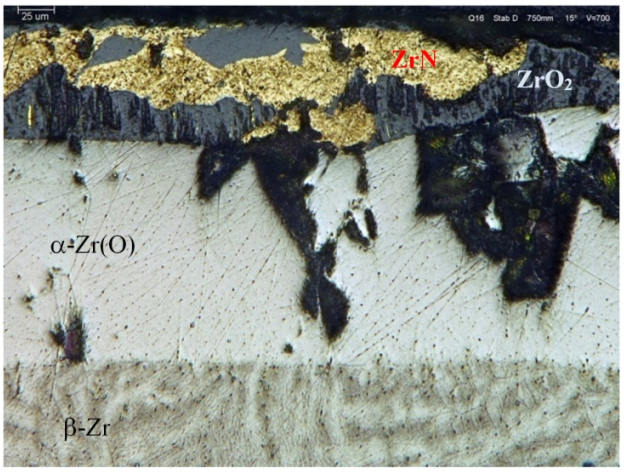

Fig. 6. Formation of nitrides at elevation of 750 mm at the end of air ingress phase.

The nitrides were formed at elevations above 350 mm under partial or full oxygen starvation conditions. If the gas phase in the gas channel contains no oxygen, the oxygen of oxide layer is transported into the metal cladding part not only from the ZrO_2/metal boundary, but also from the oxide bulk resulting in the formation of the α-Zr(O) clusters within the oxide scale[14]. The nitrogen diffused from the gas phase through the oxide scales and reacted with α-Zr(O), forming zirconium nitride clusters. No nitride formation was observed at and above elevation 950 mm with saturated α-Zr(O) layer and hence no potential for oxygen uptake from the oxide. Due to the higher density of ZrN in comparison to ZrO_2 density (ca. 25% difference), the structure of the formed nitrides is very porous.

Reflood was initiated by injecting 50 g/s of water. Almost immediately after the start of reflood there was a temperature excursion in the mid to upper regions of the bundle (500 to 1400 mm), leading to maximum measured temperatures of about 2420 K. Cooling was established at the hottest location ca. 70 s after the start of injection, but was delayed further at other locations. Reflood progressed rather slowly, due to the high temperatures and partial degradation, and final quench was achieved after about 500 s. In line with the temperature escalations, a significant quantity of hydrogen was generated during reflood (128 g) with a maximum release rate of 2.7 g/s. There are also indications of nitrogen release during the quench phase (24 g from 29 g consumed during oxygen starvation period).

IV. POST-TEST APPEARANCE

The videoscope inspection at positions of withdrawn corner rods shows an intensive degradation of the oxide layer with partial spalling at bundle elevations between 450 and 850 mm. Colored outer oxide scales (perhaps due to small nitride traces) at the surface of claddings were observed at elevations between 750 and 900 mm (Fig. 7).

Fig. 7. Post-test videoscope inspection (side view) at bundle elevation 790 mm: spalling of nitride containing oxide scales.

After videoscope investigations the bundle was filled with epoxy resin, which was hardened during two weeks. Then the bundle was cut at various elevations and the corresponding cross sections were ground and polished. Metallographic investigation of cross sections between 300 and 500 mm showed partially oxidized frozen melt (Fig. 8), relocated from upper elevations 500 – 800 mm, which could have been one important source of hydrogen during reflood.

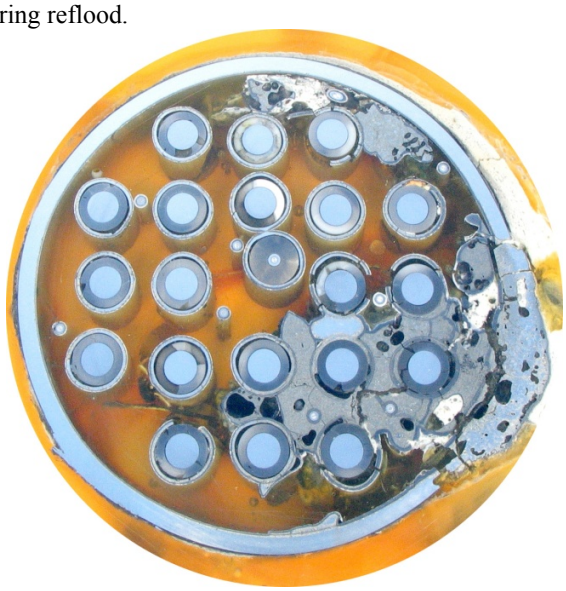

Fig. 8. Bundle cross section at 430 mm: frozen melt relocated from upper elevations.

At elevations 800 – 900 mm only local melt between pellet and outer oxide layer was observed (Fig. 9). No melt was formed at elevations above 900 mm.

Fig. 9. Bundle cross section at 830 mm: minor melting of some cladding segments.

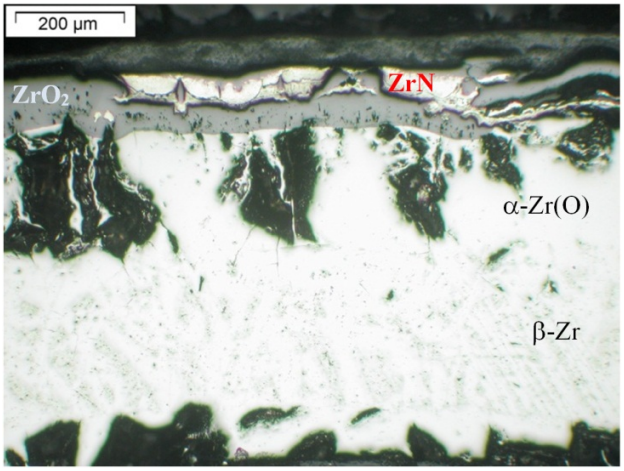

Fig. 10. Bundle elevation 350 mm, cladding of rod #5: nitrides between two oxide layers.

A very intensive nitride formation was observed at elevations 350 – 550 mm (Figs. 10 and 11). The external oxide scales above residual nitrides have a porous structure due to re-oxidation of nitrides during reflood (Fig. 11):

$$2\ ZrN + 4\ H_2O = 2\ ZrO_2 + 4\ H_2 + N_2 \qquad (1)$$

At elevations above 550 mm only some nitride traces at the boundary between the inner dense and the partially spalled outer porous oxide scales were observed. On the basis of measured nitrogen release during the quench phase (24 g) and according to formula (1), the mass of hydrogen released during nitride re-oxidation was about 7 g.

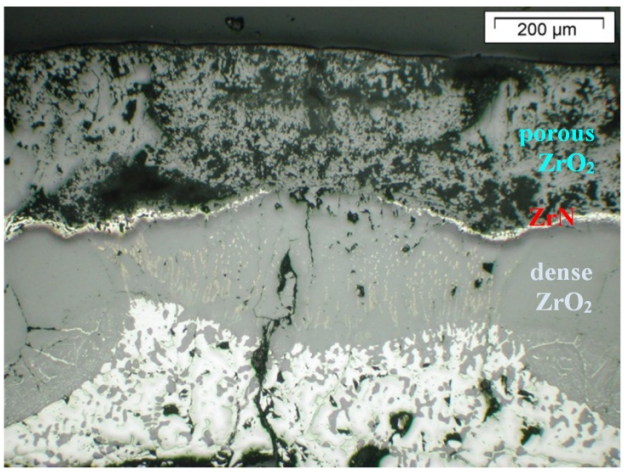

Fig. 11. Bundle elevation 550 mm, cladding of rod #9: nitrides between inner dense and outer porous oxide layers.

The image analysis of frozen melt structures (Fig. 12) allows defining the degree of oxidation of the melt on the basis of the correlation between relative area of ceramic precipitations and content of oxygen transported into the melt[15]. The average oxygen content of the melt at elevation 350 mm was measured to about 8 wt% (corresponding relative ceramic area 10%), at elevation 450 mm about 11 wt% (corresponding relative ceramic area 25%). The measurement of melt areas at different elevations allows estimating the mass of hydrogen released during the bulk oxidation of cladding melt to 19 g. Oxide scale development at the melt surface gives additionally 3 g. The similar estimation procedure for the hydrogen release during the melt oxidation of the shroud results in a mass of 3 g. Therefore, the total hydrogen production by melt oxidation is about 25 g.

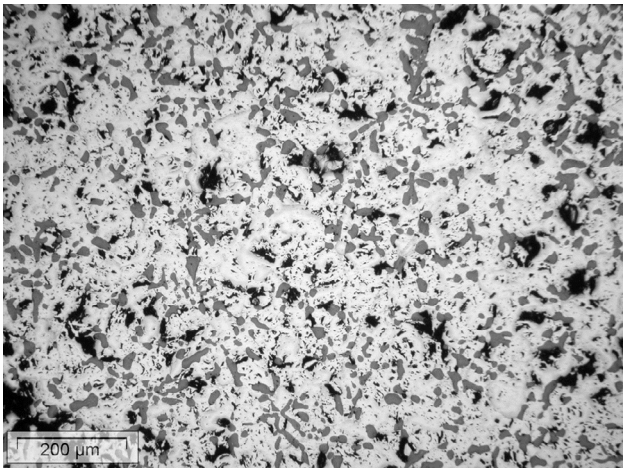

Fig. 12. Frozen Zr-O melt at elevation 450 mm: relative area of precipitations 25%.

Hence, a significant part of the hydrogen release during the quench phase can be interpreted as caused by intensive oxidation of the rod cladding and shroud metal (with formation of dense oxide sub-layer as shown in Figs. 10,11) by steam penetrated through the outer porous scale formed during the air ingress phase. The upper limit of the corresponding hydrogen amount can be estimated to 128-7-25 = 96 g.

V. SUMMARY AND CONCLUSIONS

The QUENCH-16 bundle test with Zry-4 claddings was performed with three typical features before initiation of reflood: moderate pre-oxidation to 135 µm of oxide layer (instead ca. 500 µm for QUENCH-16), a long period of oxygen starvation during the air ingress phase (ca. 800 s instead 80 s for QUENCH-10), and reflood initiation at temperatures significantly below the melting point of the cladding (ca. 1700 K instead of 2200 K for QUENCH-10).

A partial consumption of nitrogen during the oxygen starvation, accompanied by acceleration of the temperature

increase at mid bundle elevations, caused the formation of zirconium nitrides inside the oxide layer at bundle elevations between 350 and 850 mm. Due to a noticeable difference between zirconium nitride and zirconium oxide densities, the structure of formed nitride clusters is very porous.

Immediate temperature escalations after reflood initiation, leading to maximum measured temperatures of about 2420 K, were caused by massive steam penetration through the porous oxide/nitride scales and intensive reaction with nitrides and especially with metallic cladding. Very thick oxide sub-layers up to 400 µm were developed during the reflood phase. The cooling phase to the final quench lasted ca. 500 s after achievement of peak temperatures.

A relatively high concentration of residual nitrides was observed mostly at elevations 350 – 550 mm. Spalled oxide scales with a re-oxidized porous structure were observed at elevations between 350 and 850 mm.

24 g nitrogen from 29 g, consumed during oxygen starvation period, were released during the quench phase. This quantity of released nitrogen corresponds to 7 g hydrogen developed during re-oxidation of nitrides.

The total hydrogen production during QUENCH-16 was higher compared to QUENCH-10, i.e., 144 g (QUENCH-10: 53 g), 128 g of which were released during reflood (QUENCH-10: 5 g). A significant part of hydrogen released during reflood of the QUENCH-16 bundle was generated due to oxidation of the internal cladding metal layers by steam penetrated through the porous re-oxidizing nitride layer.

Metallographic investigation of cross sections between 300 and 500 mm showed partially oxidized frozen melt, relocated from upper elevations 500 – 800 mm. Image analysis of frozen Zr-O melt regions allows estimating the hydrogen release due to melt oxidation to 25 g.

ACKNOWLEDGMENTS

The LACOMECO program is performed by KIT with financial support from the HGF Program NUKLEAR and the European Commission. The authors thank all colleagues involved in the investigations, particularly J. Moch for bundle preparation, U. Stegmaier and U. Peters for metallographic analysis, J. Laier for data processing. Furthermore the very valuable support of the test planning by pre-test calculations performed at PSI, GRS, and EdF is strongly acknowledged.

REFERENCES

1. SHEPHERD et al., "Oxidation Phenomena in Severe Accidents (OPSA)", Final Report, INV-OPSA(99)-P008, 2000.

2. T. ALBIOL et al., "SARNET: Severe Accident Research Network of Excellence". ICONE-15, Nagoya, Japan, April 22-26, 2007, paper 10429. http://www.sar-net.org/upload/icone15-10429_final_sarnet.pdf

3. K. NATESAN and W.K. Soppet, "Air Oxidation Kinetics for Zr-Based Alloys", Report NUREG/CR-6846, ANL-03/32, US NRC, Washington, DC (2004). http://pbadupws.nrc.gov/docs/ML0419/ML041900069.pdf

4. L. MATUS, N. Vér, M. Kunstár, M. Horváth, A. Pintér, Z. Hózer: "Summary of separate effect tests with E110 and Zircaloy-4 in high temperature air, oxygen and nitrogen", Report AEKI-FL-2008-401-04/01 (2008).

5. M. STEINBRÜCK and M. Böttcher, „ Air oxidation of Zircaloy-4, M5 and ZIRLO cladding alloys at high temperatures", Journal of Nuclear Materials 414 (2011) 276–285.

6. M. STEINBRÜCK, Prototypical experiments relating to air oxidation of Zircaloy-4 at high temperatures, Journal of Nuclear Materials 392 (2009) 276–285.

7. http://sacre.web.psi.ch/current-projects/main-frames/documents/oecd-projects/Sandia%20Fuel%20Project%20SFP%20Description.pdf

8. Z. HÓZER, P. Windberg, I. Nagy, L. Maróti, L. Matus, M. Horváth, A. Pintér, M. Balaskó, A. Czitrovszky, P. Jani, "Interaction of failed fuel rods under air ingress conditions", Nucl. Technology, 141, p. 244 (2003).

9. J. STUCKERT, J. Birchley, C. Homann, S. Horn, Z. Hozer, A. Miassoedov, J. Moch, G. Schanz, L. Sepold, U. Stegmaier, L. Steinbock, M. Steinbrueck: "Main results of the bundle test QUENCH-10 on air ingress". 10th International QUENCH Workshop, Karlsruhe, October 26-28, 2004.

10. G. SCHANZ, M. Heck, Z. Hozer, L. Matus, I. Nagy, L. Sepold, U. Stegmaier, M. Steinbrück, H. Steiner, J. Stuckert, P. Windberg, "Results of the QUENCH-10 experiment on air ingress". Wissenschaftliche Berichte, FZKA-7087, Karlsruhe, Mai 2006. http://bibliothek.fzk.de/zb/berichte/FZKA7087.pdf

11. V.S. KONSTANTINOV, N.Y. Parshin, Y.G. Dragunov, V.V. Shchekoldin, A.E. Kiselev and T.B. Vinogradova, PARAMETR-M facility capabilities for severe accident code verification// Nuclear Engineering and Design, Volume 237, Issues 15-17, September 2007, Pages 1759-1764

12. A. KISELEV, D. Ignatiev, V. Konstantinov, D. Soldatkin, V. Nalivaev, V. Semishkin, "Main results and conclusions of the VVER fuel assemblies tests under severe accident conditions in the large-scale PARAMETER test facility". 16th International QUENCH Workshop, Karlsruhe, 16-18 November, 2010, ISBN 978-3-923704-74-3

13. A. MIASSOEDOV: "LACOMECO project within the 7th EU FWP large scale experiments on core degradation, melt retention and containment behaviour." Proceedings of the 15th International QUENCH Workshop, Karlsruhe, November 3-5, 2009. CD-ROM, ISBN 978-3-923704-71-2.

14. J. STUCKERT, M. Veshchunov, "Behaviour of Oxide Layer of Zirconium-Based Fuel Rod Cladding under Steam Starvation Conditions", Wissenschaftliche Berichte, FZKA-7373, Karlsruhe, April 2008. http://bibliothek.fzk.de/zb/berichte/FZKA7373.pdf

15. P. HOFMANN, J. Stuckert, A. Miassoedov, M. Veshchunov, A. Berdyshev, A. Boldyrev, "ZrO2 dissolution by molten zircaloy and cladding oxide shell failure. New experimental results and modeling", scientific report FZKA 6383, Karlsruhe (1999). http://bibliothek.fzk.de/zb/berichte/FZKA6383.pdf